Block-Copolymer-Free Strategy for Preparing Micelles and Hollow Spheres: Self-Assembly of Poly(4-vinylpyridine) and Modified Polystyrene

Min Wang, Ming Jiang,* Fanglin Ning, Daoyong Chen, Shiyong Liu, and Hongwei Duan

Department of Macromolecular Science and The Key Laboratory of Molecular Engineering of Polymers (Ministry of Education, China), Fudan University, Shanghai 200433, P. R. China

Received January 28, 2002; Revised Manuscript Received April 25, 2002

ABSTRACT: Noncovalently connected micelles (NCCM) with poly(4-vinylpyridine) (PVPy) as the shell and hydroxyl-containing polystyrene, i.e., PS(OH), as the core were formed in a selective solvent mixture for PVPy by inter-polymer hydrogen bonding. With increase in the hydroxyl content in PS(OH), the structure of the micelles changed from perfect spheres to rodlike and then networklike aggregates. Shell-cross-linked micelles and then hollow spheres were obtained based on the NCCM, with hydrogen bonding rather than covalent bonds between the core and shell. The shell structure was locked in by the reaction of PVPy with the cross-linker of 1,4-dibromobutane, under mild conditions. Cavitation of the spherical micelles was realized just by changing the medium from the selective solvent to a common one to dissolve PS(OH) chains in the interior of the micelles. The resultant spheres were proved to be hollow by TEM observation and by both static and dynamic light scattering. The thickness of the shell could be controlled by changing the micelle composition. DLS, TEM, SEM, and AFM studies demonstrated that the integrity of the assembled spheres was maintained during the cross-linking and cavitation. The size of the hollow spheres increased apparently with dilution of the solution. Compared to the conventional route to shell-cross-linked micelles and hollow spheres from the micelles made of block copolymers, the current approach has the significant advantages of avoiding synthesis of block copolymers and chemical degradation of the core components.

Introduction

In this paper, we report a new approach of molecular assembly to polymeric micelles and hollow spheres. This approach is novel in many aspects. First, the micelle formation is based on homopolymer/copolymer pairs by means of interpolymer complexation instead of using block copolymers, so that the specific interactions rather than chemical bonds exist between the core and shell of the micelles. Second, for producing hollow spheres, using the micelle as a precursor, simple dissolution rather than chemical degradation is used. Third, the aggregates could keep their integrity during cross-linking of the micelles and subsequent dissolution of the core component.

Inter-polymer complexes, i.e., inter-macromolecular associates of a polymer pair bound together by secondary binding forces, in particular, hydrogen bonding, have received a great deal of attention since the 1970s.[1−3] In the past decade, we found that by introducing hydrogen bonding into the polymers which originally lack donor or acceptor groups,[3] the transition from separated coils to complex aggregates took place in solution when the content of the introduced interaction sites reached a certain level. However, the complexes formed in solution are often in the form of *irregular aggregates* because each proton-donating polymer chain can interact with many donor-accepting polymer chains and vice versa. Therefore, although the complexes are products of spontaneous "molecular assembly" of the polymers, their application potential was seriously limited and consequently received much less attention than the *well-organized* polymeric molecular assemblies[4−8] such as micelles, vesicles and hollow particles.

In recent years, we have devoted effort to obtain regular assemblies, rather than irregular aggregates, based on inter−polymer complexation.[9] Two approaches have been studied. In the first, the key point is restricting one kind of the interaction sites in desired positions along a polymer chain. For example, when *carboxyl-ended* polybutadiene (CPB) and poly(4-vinylpyridine) (PVPy) were mixed in a suitable common solvent, hydrogen-bonded "graft" copolymer with PVPy backbone and CPB grafts was produced. When the common solvent was switched to a selective one, e.g., for PVPy, micelles with PVPy shell and CPB core were formed.[9c] The principle of the second approach is as follows. When a solution of polymer A is added into a solution of polymer B which is a precipitant for A, chains of A aggregate, but their precipitation can be prevented provided A and B could form interpolymer hydrogen bonding. Thus, micellelike particles with a compact A core surrounded by B shell are formed.[9d−g] Both approaches lead to noncovalently connected micelles (NCCM). Very recently, we found that the NCCM composed of a PVPy coil and *polyimide rods*, unexpectedly, formed large hollow spheres in a common solvent.[10]

In this paper, the NCCM study is extended to a polymer pair with "controllable interactions", i.e., poly{styrene-*co*-[*p*-(1,1,1,3,3,3-hexafluoro-2-hydroxylpropyl)-α-methylstyrene]} PS(OH), (Scheme 1) and PVPy. Special attention has been paid to the effects of the interaction density, which is adjustable by using PS(OH) with different hydroxyl contents, on the formation, structure, and morphologies of the micelles.

* Corresponding author. E-mail: mjiang@fudan.edu.cn.

10.1021/ma0201330 CCC: $22.00
Published on Web 06/21/2002

Scheme 1. Chemical Structure of PS(OH)

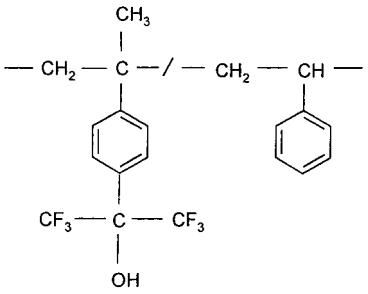

The final aim of this paper is the preparation of polymeric hollow spheres using NCCM as a precursor. Among a variety of molecular assembled structures, hollow spheres in a size range from nanometer to micrometer are particularly interesting and much in demand due to their potential uses in encapsulation of guest molecules.[11] Besides the classical approach of microemulsions to produce hollow spheres, which was described mostly in patent literature and encountered difficulties in preparing spheres of very small size, in recent years, several different routes including those based on template synthesis[12−14] and block copolymers[15−18] have been produced. The block copolymer route includes the following steps: designing and preparing a block copolymer containing a cross-linkable block and a degradable block; preparing the micelles from the copolymer in its selective solvent; locking the shell by cross-linking; and, finally, creating a central cavity by degrading the blocks contained in the core. Besides, Jenekhe et al. reported that rod−coil block copolymers could form hollow spheres via direct self-assembly in selective solvents.[8] As our present method is based on NCCM, it has significant advantages of avoiding the preparation of block copolymers and chemical degradation of the core component.

Although in this paper we concentrate on the preparation of micelles and hollow spheres from homopolymer/copolymer pairs with interpolymer hydrogen bonding *in solution*, it should be mentioned that organic materials of ordered nanometer-sized structure *in the solid state* self-assembled by small molecules due to hydrogen bonding have received much attention in the literature. Very recently Kim and co-workers[19] reported on preparing supermolecular *polymeric material* with hexagonal channels which were created by removing the template core after the formation of a cross-linked matrix.

Interpolymer Complexation between PS(OH) and PVPy in Common Solvent

The hydrogen-bonding complexation of PS(OH) with a series of proton-accepting polymers has been intensively studied,[3,20] as the hydroxyl group in $(CF_3)_2C(OH)-$ is strong in inter-association while weak in intra-association.[3,21] The counterpart PVPy is a common proton-accepting polymer, which has been employed in the studies on miscibility and complexation due to hydrogen bonding in a variety of polymer blends.[3,22] The characterization data of PVPy and PS(OH)-*X* with different hydroxyl contents are listed in Table 1. Here *X* represents the mol % of hydroxyl content in PS(OH).

Viscometry is a simple way to monitor hydrogen-bonding complexation of polymers in solution qualitatively.[3] Measurements of the relative viscosity (η/η_0) of PS(OH)-*X*/PVPy blends as a function of the composition

Table 1. Characterization Data of PS(OH)

sample code	OH content/mol %	$M_n/10^4$ g/mol	M_w/M_n
PS(OH)-1	1.0	3.7	1.51
PS(OH)-2	1.67	2.0	1.60
PS(OH)-3	3.2	4.7	1.31
PS(OH)-5	4.88	2.4	1.48
PS(OH)-12	11.7	1.9	1.50
PS(OH)-20	19.4	1.8	1.68
PS(OH)-27	27.3	1.4	1.74
PS(OH)-35	34.6	0.9	1.80
PS(OH)-42	42.0	0.5	1.92
PVPy		12[a]	

[a] Viscosity-average molecular weight.

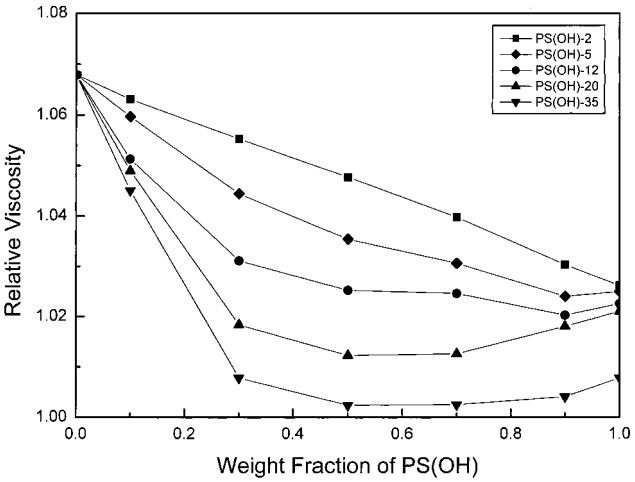

Figure 1. Relative viscosity of the blend solutions of PVPy and PS(OH)-*X* in chloroform as a function of weight fraction of PS(OH)-*X*.

were conducted by mixing solutions of PS(OH) and PVPy of the same concentration in chloroform. The appearance of the blend solutions depended on the hydroxyl content in PS(OH). The solution remained clear when PS(OH)-1, -2, and -3 were used but turned turbid, and precipitation occurred as the hydroxyl content reached and exceeded 5 mol %. The measurements were conducted 10 min after mixing the solutions for the former case while filtration of the solutions was done prior to the measurements for the latter.

Figure 1 shows the variation of the relative viscosity of PS(OH)/PVPy blend solutions in chloroform as a function of weight fraction of PS(OH). For the blends with hydroxyl contents being 1, 2, and 3, the viscosity changed smoothly, and is close to the corresponding values calculated by the additivity rule (for clarity, curves of PS(OH)-1 and PS(OH)-3 are not shown). As the total concentration of polymers in the blend solution is 3.0×10^{-3} g/mL, much lower than its overlap concentration C^*, obeying the additivity law may mean that the component coils keep independent and no substantial complex formed.

When the hydroxyl contents reached 5 mol %, the viscosity profile of the blend solutions showed an apparent negative deviation from the additivity. This indicates the chains collapsed and partially precipitated due to interpolymer complexation. When the hydroxyl content increased further, the visicosity decreased dramatically. Being an extreme, the viscosity of PS(OH)-35/PVPy blend solution displays a minimum close to that of pure solvent, indicating that nearly all the component polymers precipitated as complexes.

Laser light scattering (LLS) has proved to be more sensitive than viscometry in investigating association

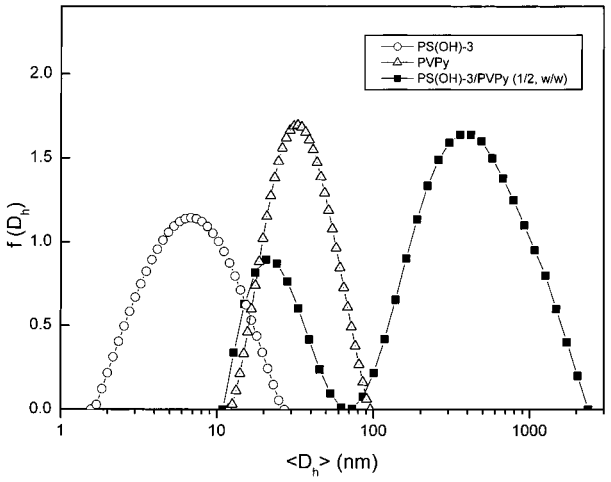

Figure 2. Hydrodynamic diameter distributions of PVPy, PS(OH), and PS(OH)-3/PVPy (1/2, w/w) in chloroform. The total concentration of polymers is 1.0×10^{-4} g/mL.

and aggregation process, especially in very dilute solutions.[3,22c] Figure 2 shows the hydrodynamic diameter ($\langle D_h \rangle$) distributions of PS(OH)-3, PVPy, and their blend solutions with total concentrations of polymers of 1.0×10^{-4} g/mL. For PS(OH)-3, the peak is below 10 nm; for PVPy, the peak is located at about 30 nm. It is interesting to note that the distribution of PS(OH)-3/PVPy are bimodal. Besides the small peak located at about 20 nm, which is obviously attributed to the individual component polymers in solution, a large peak associated with polymer aggregates in a size range around 400 nm appeared. This is a direct evidence of complex formation in PS(OH)-3/PVPy. As dynamic light scattering (DLS) is very sensitive to large particles, the relative small peak area of the independent coils does not mean that the number of the individuals is smaller than that of the complex.

Although DLS proved the presence of the PS(OH)-3/PVPy complex, the blend solution remained clear and showed no precipitate formation. As in PS(OH)-3, on average, there is only one hydroxyl group per 30 styrene units, when hydroxyl interacts with pyridyl on PVPy, the inert PS sequence between two neighboring hydroxyls will form loops or dangling chains, leading to a loose structure. When hydroxyl contents in PS(OH) increased to 5 mol % or more, the complexes gradually lost their solvation ability due to forming a segment-pairing structure.

Micelle Formation and its Morphology

As the formation of interpolymer complexation in solution often leads to an irregular precipitate, in order to allow a complementary polymer pair to assemble into micelles, one needs to use a selective solvent so that the hydrogen bonding between the component polymers is allowed to occur on the core−shell interface area mostly. PS(OH) and PVPy differ substantially in their solubility behavior. Chloroform was a good solvent for both, while nitromethane was found to be a good solvent for PVPy but a nonsolvent for PS(OH). Therefore, the mixture of $CHCl_3/CH_3NO_2$ (v/v, 1/9) was used as a selective solvent for preparing the NCCM composed of PS(OH) core and PVPy shell. When a dilute solution of PS(OH) in $CHCl_3$ was added into nitromethane, precipitation occurred immediately. However, no precipitation was found as the solution was added into nitromethane containing PVPy; instead, a bluish tinge appeared. Obviously, the aggregates of PS(OH) were stabilized by the solvated PVPy chains which are attached to the aggregate surface by hydrogen bonding between the pyridine ring and hydroxyl in PS(OH). This procedure has been used to prepare stable PS(OH)/PVPy micelles in $CHCl_3/CH_3NO_2$ (v/v, 1/9).

Table 2. Preparation Conditions and Compositions of the Micelles (M), Cross-Linked Micelles (C) and Hollow Micelles (H)

micelle code	PS(OH)-*X*	C/PS(OH) × 10^3 g/mL	C/PVPy × 10^3 g/mL	composition PS(OH)/PVPy (w/w)
M1 (M6)	2	4 (8)	0.2	2.2/1 (4.4/1)
M2 (M7)	12	4 (8)	0.2	2.2/1 (4.4/1)
M3 (M8)	20	4 (8)	0.2	2.2/1 (4.4/1)
M4 (M9)	27	4 (8)	0.2	2.2/1 (4.4/1)
M5 (M10)	42	4 (8)	0.2	2.2/1 (4.4/1)
M11 (M12)	12	1.2 (9)	0.2	0.67/1 (5.0/1)
M13 (M14)	20	1.2 (9)	0.2	0.67/1 (5.0/1)
M15	2	10.75	0.5	2.4/1
M16	12	8	2.0	0.44/1
C15	cross-linked micelle from M15			
H15	hollow spheres from C15			
C16	cross-linked micelle from M16			
H16	hollow spheres from C16			
H8	hollow spheres from C8			

There are many factors affecting the assembly of PS(OH) and PVPy, i.e., hydroxyl content in PS(OH), initial concentrations of PS(OH) and PVPy, final composition, temperature, and even the mixing procedure and speed etc. As we are mainly interested in the effect of the interaction density between PS(OH) and PVPy, a series of micelle solutions containing PS(OH)-*X* with *X* ranging from 2 to 42 mol % at a given initial concentration were prepared by adding PS(OH)/$CHCl_3$ into PVPy/CH_3NO_2 very slowly (Table 2). The morphologies of the micelles (M1−M5) were observed by TEM as shown in Figure 3. In this paper, the micelles, cross-linked micelles and hollow spheres are denoted as M, C, and H respectively (Table 2).

Figure 3a displays the morphologies of M1 composed of PS(OH)-2/PVPy. It is interesting to find that the individual micelles are spherical, and most of them are in the diameter range of 35−50 nm. As no core−shell structure is observed and the circular outline seems distinct and perfect, we are inclined to think that the spheres observed correspond to the micelle core, and the shell of PVPy is not discernible as the chain density is too low.[15c,23]

The morphologies of M2 containing PS(OH)-12 in Figure 3b resemble that of M1 in both the contour shape and size range. As the hydroxyl content increases to 20 mol % (M3), an apparent variation in morphology takes place; i.e., spheres turn to ellipsoids and even wormlike or short rods (Figure 3c). It is noticeable that the diameter of the cross sections of the wormlike structures or rods is similar to that of the large spheres, i.e., about 40 nm. Furthermore, the morphologies of PS(OH)27/PVPy micelles (M4) shown in Figure 3d are characteristic of the coexistence of spheres, ellipsoids, and micronetworks composed of the short rods. Besides, the cross section size of the short rods decreases significantly to about 20−30 nm only. Finally, as the hydroxyl content increases to 42 mol % (M5), i.e., on average, there is one interaction site per 2−3 PS(OH) monomer units, most of the micelles are in the shape of short rods

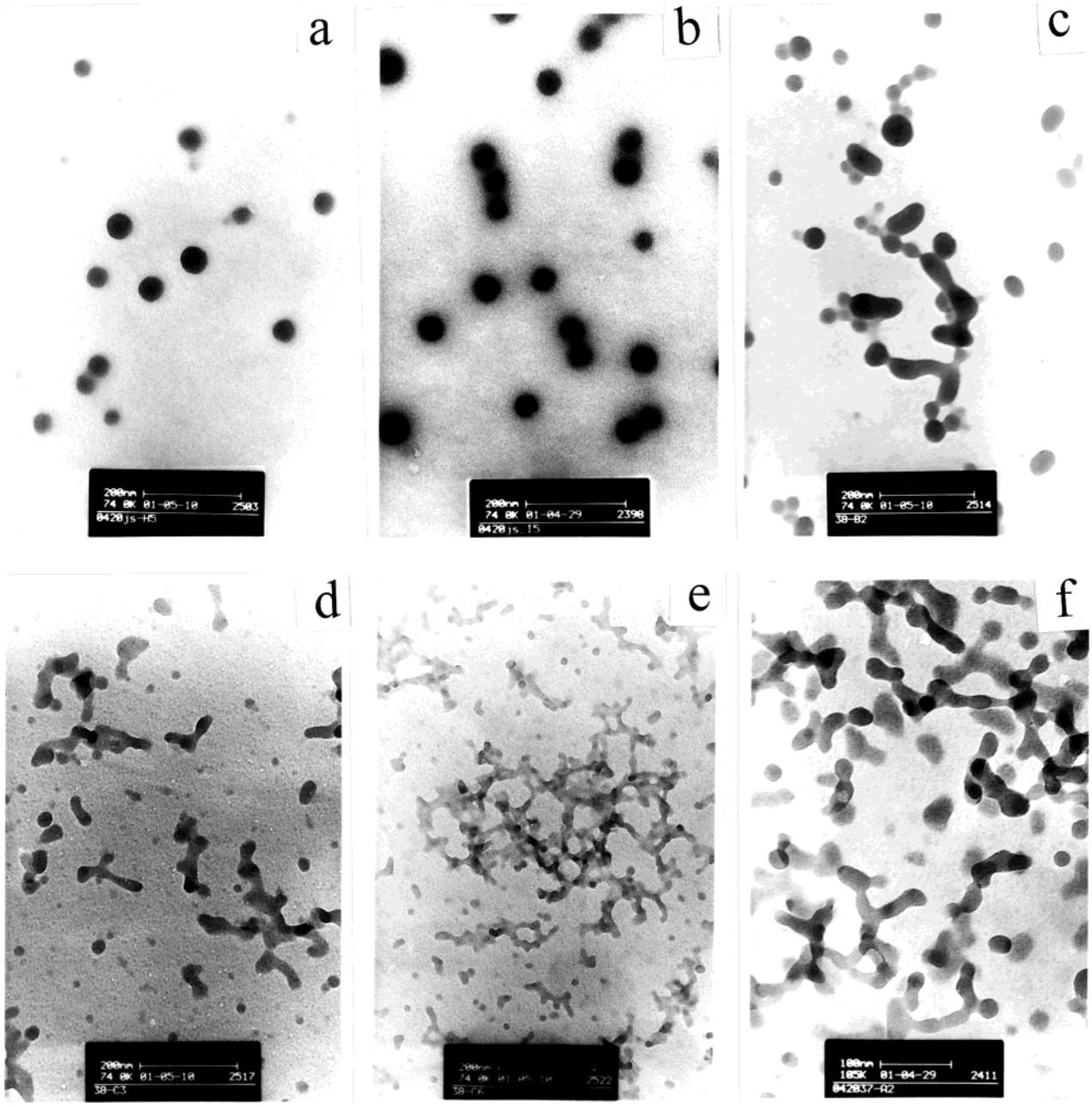

Figure 3. TEM micrographs of (a) M1, (b) M2, (c)M3, (d) M4, (e) M5, and (f) M8.

and some of them combine together to form relatively large networks extending to 500 nm. In addition, the transverse size of the short rods decreases further, to about 15−25 nm (Figure 3e).

In short, Figure 3a−e displays a regular change in the micellar morphologies with the hydroxyl content in PS(OH). The trends are clear, i.e., with increasing hydroxyl content and consequently intensifying interactions between the two components, the diameter or transverse size of the micelles, i.e., spheres or rods, gradually decreases, and at the same time, the elementary micelles show an increasing ability to combine into clusters or networks. This variation of the aggregate morphologies with the hydroxyl content in PS(OH) is illustrated schematically in Figure 4.

As reported in the previous section, in a common solvent, PS(OH) and PVPy turned turbid and complex precipitation occurred when the hydroxyl content in PS(OH) reached 5 mol % or more. In the procedure of micelle preparation, rapid aggregation of PS(OH) generally prevented sufficient interaction between the hydroxyl and pyridine groups, so that no macroscopic precipitation of the complex took place. Furthermore, we have reasons to believe that, for the cases with higher density of the interaction sites, the aggregation of PS(OH) was accompanied by incorporating PVPy chains. So the aggregates probably did not have a well-defined core−shell structure, but the two components interpenetrated each other with enrichment of PVPy on the surface area as schematically shown in Figure 4. This hypothesis is supported by the successive studies of cross-linking and cavitation.

Micellar Variation with Hydroxyl Content Monitored by DLS

As DLS is able to measure the translational diffusion coefficient of particles in solution and hence $\langle D_h \rangle$ of the corresponding equivalent hydrodynamic spheres, it has

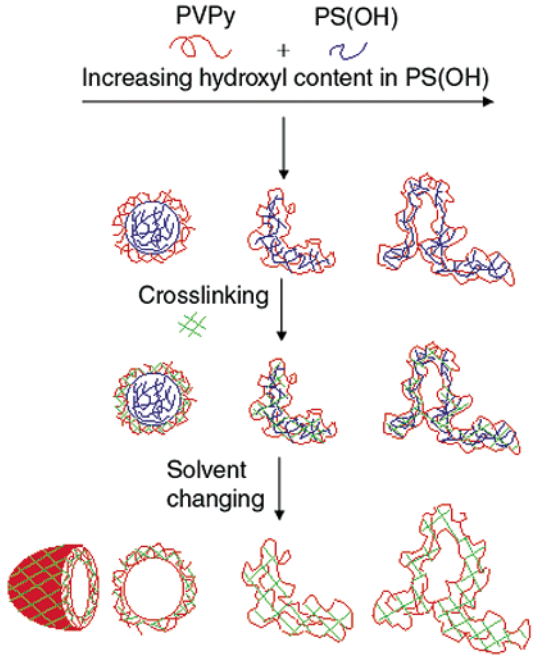

Figure 4. Schematic illustration of the variation of the aggregate morphologies with the hydroxyl content in PS(OH).

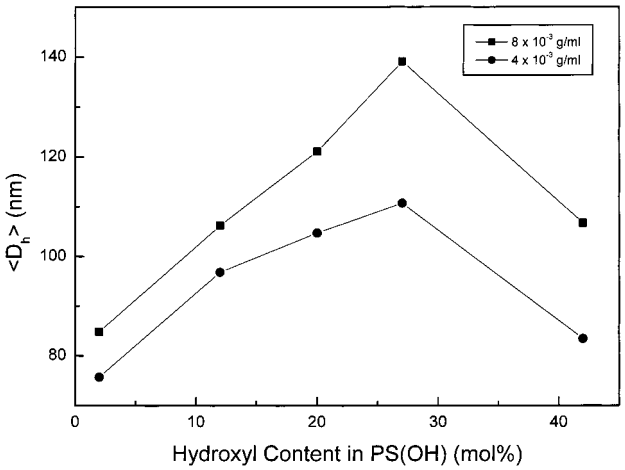

Figure 5. $\langle D_h \rangle$ of PS(OH)/PVPy micelles as a function of hydroxyl content in PS(OH) in chloroform/nitromethane (1/9, v/v).

been widely used in the studies of polymeric micelle solutions.[9c,9d,24] In the present study, attempts have been made to explore the effect of the interaction density between the two component polymers on the character of the formed micelles. As reported above, spherical micelles were obtained only when the hydroxyl content in PS(OH) was low (2−12 mol %), while the high hydroxyl content in PS(OH) resulted in complex structures having significant asymmetry in shape and broad size distributions. Therefore, we could not expect a quantitative explanation from DLS, although these results provide interesting information to corroborate the transmission electron microscopy (TEM) observations.

Figure 5 shows the variation of $\langle D_h \rangle$ of PS(OH)/PVPy aggregates as a function of hydroxyl content in PS(OH). The lower and upper curves refer to the micelle groups of M1−M5 and M6−M10, which were obtained from different concentrations of PS(OH) and consequently, different final compositions, i.e., PS(OH)/PVPy of 2.2/1 and 4.4/1 w/w, respectively (Table 2). The two curves

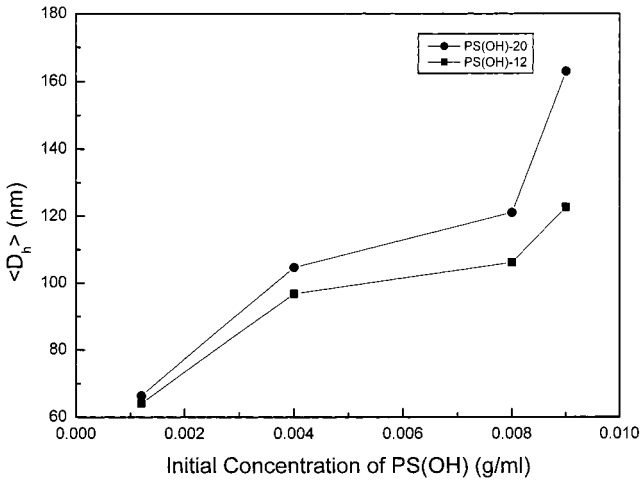

Figure 6. $\langle D_h \rangle$ of PVPy/PS(OH) micelles in chloroform/nitromethane (1/9, v/v) as a function of initial concentration of PS(OH) (or final composition of the micelles).

present similar trends, i.e., $\langle D_h \rangle$ increases significantly with hydroxyl content in PS(OH) over a broad range but decreases as the content reaches very high values (27−42 mol %). The morphologies shown in Figure 3a−e correspond to the aggregates in the lower curve (M1−M5) and only that shown in Figure 3f is for the PS(OH)-20/PVPy aggregates (M8) in the upper curve. The $\langle D_h \rangle$ values of M1 and M2 are much larger than those observed by TEM because the shell, or at least the outer part of the shell, is invisible in TEM. For the cases of PS(OH) with hydroxyl contents higher than 12 mol %, as the micelles deformed and the short rods aggregated further, the sizes calculated from the translational diffusion coefficient actually reflected the behavior of micelle aggregates or clusters as an entirety. Therefore, the increase of $\langle D_h \rangle$ with hydroxyl content over the range from 2 to 27 mol % is in accordance with the morphology change shown in Figure 3a−d rather than the transverse size of the individual short rods. The decrease of $\langle D_h \rangle$ in the very high hydroxyl content range, i.e., from 27 to 42 mol %, may reflect that the peripheral shape of the aggregate composed of the short rods becomes more highly branched causing a decrease of the outline size.

A comparison between the two curves for two groups of solutions i.e., M1−M5 and M6−M10, shows clearly the effect of the initial concentration of PS(OH). A 2-fold concentration of PS(OH) causes a substantial increase in $\langle D_h \rangle$. For example, $\langle D_h \rangle$ of PS(OH)-20/PVPy from the low (4×10^{-3} g/mL) and high (8×10^{-3} g/mL) concentration are 102 and 121 nm, respectively. The corresponding difference in the morphologies can be seen by comparing parts c and f of Figure 3.

Figure 6 shows the $\langle D_h \rangle$ variation over a broad range of the initial concentration of PS(OH) and accordingly the final composition. Generally, in both cases of PS(OH)-12 and PS(OH)-20, the micellar size significantly increases with the concentration of PS(OH). The result is readily understandable, as at higher PS(OH) concentrations collapse and aggregation of the PS(OH) chains becomes more rapid when the medium surrounding the chains becomes poor. Increasing the PS(OH) concentration at a given concentration of PVPy results in an increase in the micelle size. As the D_h distribution curves for all the micelle solutions prepared at these concentration ranges of PS(OH) and PVPy show no

Table 3. Dependence of Micelle Size and Polydispersity on Preparation Procedures

proc[a]	PS(OH)-*X*	C/PS(OH) × 10^3 g/mL	C/PVPy × 10^3 g/mL	$\langle D_h \rangle$ (nm)	polydispersity
A	20	3	0.5	66	0.24
B	20	3	0.5	62	0.14
A	27	5	0.5	97	0.29
B	27	5	0.5	73	0.20

[a] In procedure A, the micelle is prepared by adding PS(OH)/$CHCl_3$ into PVPy/CH_3NO_2 solutions, while in procedure B, it is prepared by adding PVPy solution into PS(OH) solution.

signals associated with individual PS(OH) and PVPy chains (curve not shown), we may say that most of the component polymers have assembled into the micelles. In other words, for current NCCM, the micelle composition, i.e., the weight or volume ratio of the core to shell, is readily adjustable over a certain range by just changing the feed composition.[9c] This provides NCCM a significant advantage over the micelles made of block copolymers, in which the composition adjustment highly depends on synthesis, which in most cases is costly and time-consuming.

All the micelles of M1−M10 were prepared by adding PS(OH)/$CHCl_3$ solutions into PVPy/CH_3NO_2 (procedure A). It is worth noting that the micelles prepared by the opposite way, i.e., procedure B, adding PVPy/CH_3NO_2 into PS(OH)/$CHCl_3$ solutions resulted in a smaller and narrower distribution. Table 3 presents two examples. This is understandable as in procedure B the degree of solvation of PS(OH) chains worsens much slowly than in procedure A; thus, the PS(OH) chains have more chance to interact with and be stabilized by PVPy chains. In fact, despite the mixing method of the component solutions, the micelles or aggregates of PS(OH)/PVPy are in essence kinetically trapped morphologies.

Shell-Cross-Linking and Cavitation of Micelles

The procedure for producing hollow spheres includes locking the structure in by cross-linking the shell and then dissolving the core. Two examples, obtaining "thin shell" and "thick shell", respectively, are described as follows.

A thin-shell sphere (M15) was prepared by the procedure A with a composition of PS(OH)-2/PVPy 2.4/1. As both initial concentrations of PS(OH)-2 and PVPy are larger than the corresponding ones in preparing micelles M1−M10 with similar compositions, larger micelles with $\langle D_h \rangle$ of 152 nm and polydispersity of 0.21 were obtained. (Figure 7).

1,4-dibromobutane was selected as cross-linker.[25,26] Then 50 mol % of 1,4-dibromobutane based on the pyridine units was added into the solution of M15 and the mixture was kept at 60 °C for 2 days. In a control experiment, the micelle solution without adding the cross-linker was treated at the same conditions. After the reaction, DLS measurement indicated a slightly smaller diameter of 138 nm for the cross-linked micelle C15 (Table 2). This means that the shell structure was successfully locked in, which is called SCK's.[27] Adding an equivolume of dimethylformamide (DMF) into the solution, which not only could solubilize both components but also could cause dissociation of the interpolymer hydrogen bonding leading to decomplexation,[3,22c] led to a significant increase of the $\langle D_h \rangle$ up to 194 nm (Figure 7), while for the control, micelles disappeared as monitored by DLS. The size expansion of a micelle

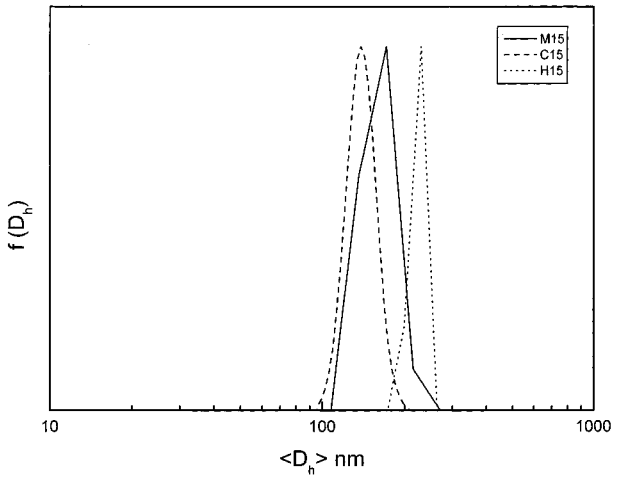

Figure 7. Hydrodynamic diameter distributions of M15, C15, and H15.

Table 4. Size Dependence of the Hollow Spheres on Concentration

H15	C ($\times 10^4$ g/mL)	2.25	0.583	0.229	0.141
	$\langle D_h \rangle$ (nm)	194	224	226	268
H16	C ($\times 10^4$ g/mL)	9	0.363	0.257	0.189
	$\langle D_h \rangle$ (nm)	123	167	176	188

caused by removing the species contained in its interior was reported previously.[16b,17] In the case of block copolymer micelles, this expansion is of course a result of releasing the restriction imposed by the insoluble blocks aggregated in the core on the solvated blocks. The same phenomenon found for our NCCM reflects the restriction on the PVPy chains caused by the aggregated PS(OH). Another reason for this expansion, i.e., increasing the solvation power of the medium for the PVPy nanocage by adding DMF cannot, of course, be excluded.

We found that the apparent $\langle D_h \rangle$ of the hollow spheres H15 substantially increases with diluting the solutions with the mixed solvent of chloroform/nitromethane/DMF (v/v/v, 1/9/10). Specifically, as the concentration varied from 2.25×10^{-4} to 0.141×10^{-4} g/mL, the diameter increased from 194 to 268 nm and accordingly, the spherical volume expanded by a factor of 2.7 (Table 4). This is a very interesting phenomenon and has not been reported and investigated previously. The finding implies that the degree of swelling of the nanocage or membrane in the shell can be controlled by adjusting the concentration and it could be very high at extremely dilute solutions. The micelles having controllable cavities were demonstrated further by a combination of static light scattering (SLS) and DLS. The above solutions of H15 in the solvent of chloroform/nitromethane/DMF (v/v/v, 1/9/10) were measured by SLS giving an apparent molecular weight of 1.09×10^7 and radius of gyration $\langle R_g \rangle$ of 146 nm. Also, $\langle D_h \rangle$ obtained by DLS in an extremely dilute solution ($C = 1.4 \times 10^{-5}$ g/mL) was 268 nm. Therefore, we found that apparent density of the spheres are 1.8×10^{-3} g/mL ($\rho = M_w/N_A(4/3)\langle R_h \rangle^3$, where N_A is Avogadro's number), which is about 2 orders of magnitude smaller than the ordinary polymer micelles[24] and surfactant-free dispersed polymer particles.[28] This low density is of course in accordance with the model of hollow spheres. In addition, the $\langle R_g \rangle/\langle R_h \rangle$ value of 1.09 is far different from the expected theoretical values[29] for a uniform sphere (0.774) and a polymer coil (1.50) but fairly close to that for nondraining thin layer hollow spheres (∼1.0).

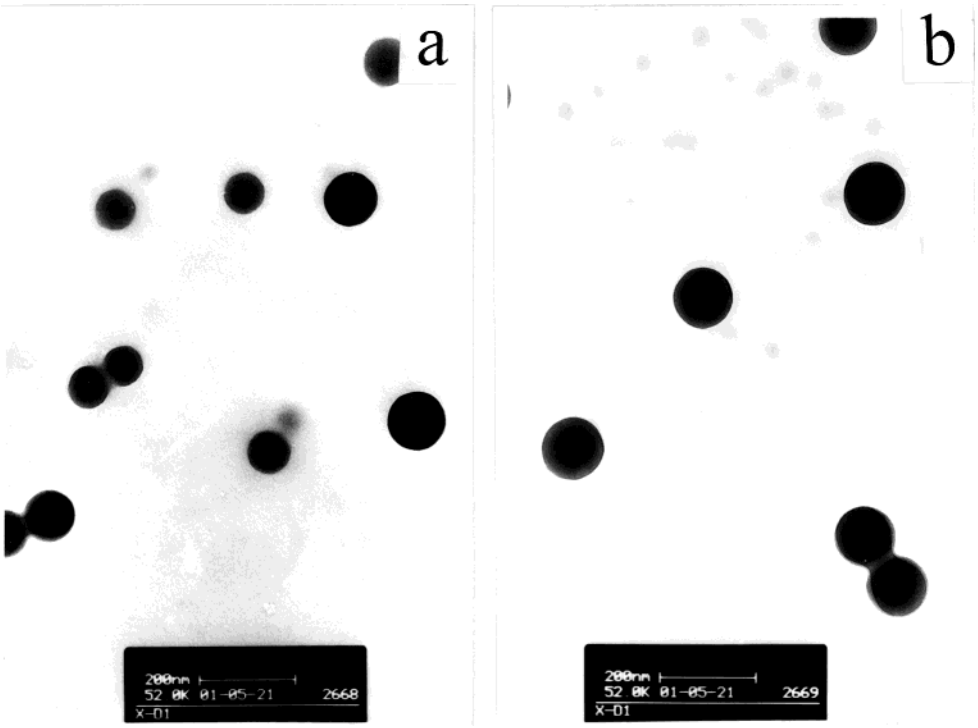

Figure 8. TEM micrographs of (a) M15 and (b) C15.

The "thick shell" micelles M16 with a composition of PS(OH)-12/PVPy (0.44/1), i.e., the weight fraction of the shell being 0.7, was prepared by a similar method but with a high initial concentration of PVPy. The $\langle D_h \rangle$ of the thick-shell micelle was measured to be 95 nm. After cross-linking, it changed to 87 nm (C16). Removing the core by adding equivolume of DMF to the solutions of C16 resulted in larger hollow micelles with a $\langle D_h \rangle$ of 123 nm (H16). It was also observed that the micelle size increased with dilution as $\langle D_h \rangle$ reached as high as 188 nm at an extremely dilute concentration of 1.89×10^{-5}g/mL (Table 4). Meanwhile, SLS gave an apparent molecular weight of 6.66×10^6 and $\langle R_g \rangle = 96$ nm. Therefore, we found that $\langle R_g \rangle / \langle R_h \rangle$ is 1.02 and the average density is 3.2×10^{-3} g/mL. Once again, these data support the model of hollow spheres. In addition, this density of the "thick shell" is apparently larger than that of the "thin shell".

In short, DLS and SLS studies demonstrated that we have successfully designed and performed a method for preparing NCCM and based on which, the SCK's with immobile but permeable cross-linked peripheral shell and finally, hollow spheres by simply dissolving the polymer chains contained in the interior of SCK's.

Morphology of Hollow Sphere

TEM, scanning electron microscopy (SEM), and atomic force microscopy (AFM) have been used to explore the morphological variation of the NCCM caused by the shell-cross-linking and subsequent core-removal. TEM is capable of examining the internal structure of the aggregates while AFM and SEM allow for visualization of three-dimensional shape.

The morphologies of the M15 micelles and its cross-linked product C15 are shown in Figure 8, parts a and b, respectively. As the number of the micelles is not large enough, accurate evaluation of average diameter and its distribution cannot be carried out. However, compared to M1 shown in Figure 3a, M15, which were prepared by using higher initial concentrations, possesses larger diameters. In addition, the microphotographs clearly show the perfect spherical shape of both the micelles M15 and C15. In other words, the spherical micelles maintained their integrity during the cross-linking reaction, and in particular, no intermicelle fusion took place.

A dramatic morphological change for C15 caused by adding equivolume DMF into its solutions in chloroform/nitromethane (v/v, 1/9), has been explored by TEM. A remarkable feature of the micrographs shown in Figure 9, parts a and b, is the obvious contrast between the periphery and center in most of the spheres. This feature is characteristic of the projection images of hollow spheres.[10,12a,30,31] The results demonstrate that the PS(OH)-2 chains have been removed from the interior of the micelles simply by changing the medium without any chemical degradation. The micrographs display micellar aggregates rather than individual particles. This aggregation probably took place during solvent evaporation during the preparation of TEM specimens, as DLS measurements for the C15 and H15 solutions indicate smaller particle sizes in accordance with the individual spheres. A close examination of the micrograph provides a relatively rough evaluation of the ratio of the outer radius R to the inner radius R_i of the shell being about 1.10. Thus, the volume ratio of the shell to the core $(R/R_i)^3 - 1$, would be 0.33. This value is close to the weight ratio of PVPy to PS(OH) in M15, i.e., 0.42. In addition, we noticed that a minority of spheres do not show the hollow structures but rather uniform contrast over the spheres. For these particles, perhaps the local cross-linking density is too high to remove the PS(OH) chains. The exact reasons for this coexistence of hollow spheres and homogeneous ones remains unclear.

The three-dimensional morphology of H15 was studied by AFM on mica substrate. As clearly shown in Figure 9c, most hollow spheres are individual particles

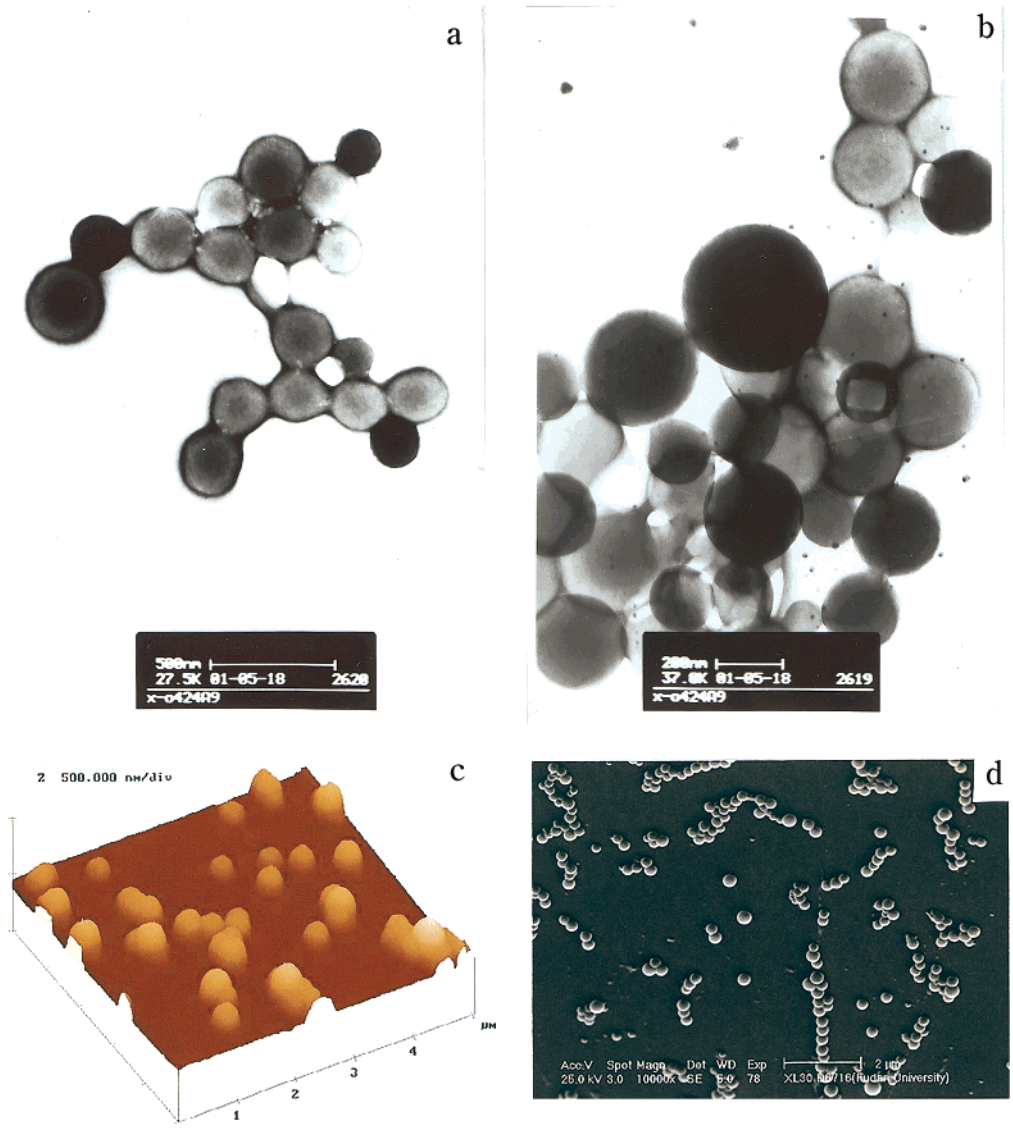

Figure 9. Micrographs of hollow spheres: (a and b) TEM of H15, (c) AFM of H15, and (d) SEM of H15 observed using sample stage with tilting angle 40°. Both were prepared in chloroform/nitromethane/DMF (1/9/20, v/v/v).

without substantial interparticle fusion. More importantly, differing from the morphologies of hollow spheres made from block copolymers showing flattened or collapsed spreading structure,[16b,17] the present spheres are standing on the substrate. In other words, the hollow spheres made of cross-linked poly(4-vinylpyridine) shells are shape-persistent, thus maintaining their integrity. This integrity persistence was confirmed by SEM observations as all the particles keep their spherical shape even after vacuum-drying. This superior mechanical property of the hollow spheres is perhaps caused by a relatively larger chain density of the shell compared to that of the ordinary micelles of block copolymers in which one insoluble block connects one soluble chain only. This valuable property of the shell may well provide significant advantages in encapsulation applications of such hollow spheres.

The same procedure for preparing hollow structures from the micelles with high hydroxyl contents in PS(OH) was performed as well. One example is based on M8 with PS(OH)-20/PVPy 4.4/1. (Figure 3e) After cross-linking and changing the solvent for removing soluble PS(OH)-20 takes place, the final structure is shown in Figure 10. The short-rod shape completely disappeared and was replaced by irregular aggregates with loose structure. This irregular structure is of course composed of cross-linked PVPy. This result supports our opinion regarding the structure of the aggregate mentioned above; namely, for the aggregates containing PS(OH) with high hydroxyl content, there is probably no clear core−shell structure, and instead, PVPy and PS(OH) interpenetrate each other. Therefore, cross-linking and the subsequent dissolution of PS(OH) resulted in irregular loose structures. This change in morphology of the hollow bodies with increasing hydroxyl content in PS(OH) is also schematically shown in Figure 4. This result indicates that the core−shell structure of NCCM is an important premise for the preparation of the desired hollow structures.

M16 is a micelle with "thick shell", which was demonstrated by LLS studies. However, we failed to confirm the presence of an inner cavity for H16 by TEM observations. In fact, the differences in the electron scattering between passing through the central part and shell part becomes less as the shell thickness increases. In the present "thick-shell" case, this difference turns to be too small to present a discernible contrast. Similar results were reported for the hollow spheres, in which

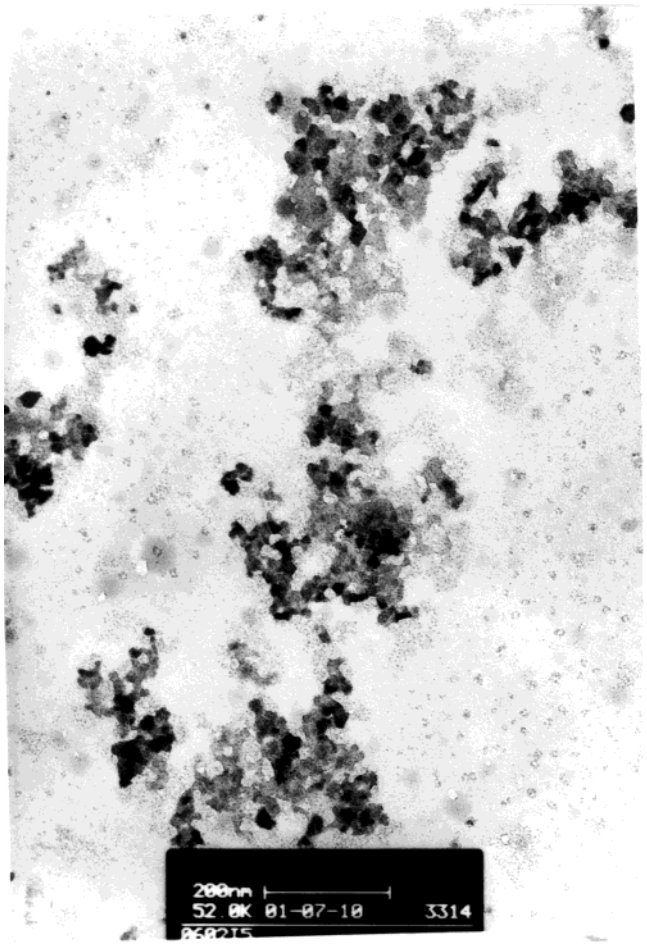

Figure 10. Micrograph of H8.

the cavity was created by ozonolysis of polystyrene blocks.[15c]

Experimental Section

Measurements. ^{1}H NMR spectra were acquired on a Bruker AMX-400 NMR spectrometer with tetramethylsilane as the internal standard. FTIR spectra were obtained on a Nicolet Magna 550 spectrophotometer as KBr pellets.

Size exclusion chromatography (SEC) measurements were conducted using a Waters model 510 HPLC Pump and an ERMA ERC-7512 refractive index detector, and a set of columns from Polymer Standard Service. Calibration was carried out with polystyrene standards. THF as eluent at a flow rate of 1.0 mL min^{-1} was used and the fluorine content of the copolymers (PS(OH)) was measured by anionic chromatography using a Dionex 2110I.

Measurements of the relative viscosity (η/η_0) of the blend solutions in chloroform were made as a function of composition using an Ubbelodhe viscometer at 30.0 ± 0.1 °C. The original concentrations of the component polymers were 3.0×10^{-3} mg/mL.

A commercial laser light scattering (LLS) spectrometer (Malvern Autosizer 4700) equipped with a multi-τ digital time correlation (Malvern PCS7132) and a solid-state laser (ILT 5500QSL, output power = 100 mW at $\lambda_0 = 514.5$ nm) as light source was used. The measurements were preformed at 30.0 ± 0.1 °C, where the relative error of $\langle D_h \rangle$ is less than 2%. The solutions were respectively clarified using a 0.45-μm Millipore filter before the measurements and then poured into the cell. In DLS, the line-width distribution $G(\Gamma)$ can be calculated from the Laplace inversion of the intensity−intensity−time correlation function $G^{(2)}(q,t)$.[32] The inversion was carried out by the CONTIN program supplied with the Malvern PCS7132 digital time correlator. $G(\Gamma)$ can be converted into a translational diffusion coefficient distribution $G(D)$ or a hydrodynamic diameter distribution $f(D_h)$ via the Stokes−Einstein equation, $D_h = (k_B T/3\pi\eta)D^{-1}$, where k_B, T, and η are the Boltzmann constant, the absolute temperature, and the solvent viscosity, respectively.

TEM was performed on a Philips CM 120 electron microscope at an accelerating voltage of 80 kV. The specimens were prepared by placing 5 μL micelle solutions on copper grids coated with a thin carbon film and allowing them to dry freely.

SEM and AFM were conducted with a Philips XL30 and Nanoscope III-microscopes, respectively. The sample preparation for SEM was similar to that for TEM. Samples for AFM imaging were prepared by placing a 5 μL drop of micelle solution on freshly cleaved mica and allowing it to dry in a desiccator.

Materials. Poly(4-vinylpyridine) was synthesized by free radical polymerization of 4-vinylpyridine (Aldrich) which was distilled from CaH_2 three times. The viscosity-average molecular weight of the polymer (M_η) of the polymer was 1.2×10^5. The hydroxy-containing monomer *p*-(hexafluoro-2-hydroxyisopropyl)-α-methylstyrene (HFMS) was synthesized from 4-chloro-α-methylstyrene via a Grignard reaction with hexafluoroacetone. Both IR and NMR confirmed the existence of HFMS: IR 3600, 3520, 1629, 1611−1513, 1150−1126 cm^{-1}; NMR δ 2.0 (CH_3, 3H), δ 4.0−5.0 (−CH, 1H), δ 4.9−5.2 (H in double bond, 2H), δ 7.0−8.0 (aromatic ring, 4H). Random copolymers of styrene and HFMS (PS(OH)) were synthesized and purified as described previously.[33] By variation of the feed composition, a series of PS(OH) samples with the HFMS content ranging from 1.0 to 42 mol % were produced. The HFMS content in PS(OH) was determined by fluorine analysis. The molecular weight of PS(OH) samples were measured by SEC. All the results are listed in Table 1. The samples were denoted by PS(OH)-*X* where *X* represents the HFMS content (in mol %).

Formation of Micelles. To prepare the micelle solution, PVPy and PS(OH) were dissolved in nitromethane and chloroform separately. To prepare M1−M5, 1 mL PS(OH)-*X*/chloroform solutions (4×10^{-3} g/mL) were added dropwise very slowly (ca. 0.2 mL/min) into 9 mL PVPy/nitromethane solutions (0.2×10^{-3} g/mL). The solutions turned from completely colorless and transparent to slightly bluish, indicating the formation of micelles. The mixture was stirred for ca. 24 h at room temperature and then kept for 5 days before measurements. DLS and TEM were used to characterize the micelle solutions. M6−M16 were prepared via the same procedure but with different polymer concentrations as listed in Table 2.

Shell-Cross-Linking of Micelles. To the micelle solution of PS(OH)/PVPy was added a 50 mol % of cross-linker 1,4-dibromobutane based on the pyridine units. The reaction mixture was stirred for 48 h at 60 °C. The average hydrodynamic diameter $\langle D_h \rangle$ was determined by DLS, and the morphology of the micelles was detected by TEM.

Cavitation of Shell-Cross-Linked Micelles. To one volume of the shell-cross-linked micelle solution was added one volume of DMF. The mixture was stirred for 12 h at room temperature and kept for 5 days before measurements. The micelle solutions were characterized by LLS, TEM, SEM, and AFM.

Acknowledgment. This work was supported by the National Natural Science Foundation of China (NNSFC No.29992590, 50173006) and the National Basic Research Project-Macromolecular Condensed State Program.

References and Notes

(1) Tsuchida, E.; Abe, K. *Adv. Polym. Sci.* **1982**, *45*, 1.
(2) Bekturov, V.; Bimendina, L. *Adv. Polym. Sci.* **1981**, *41*, 99.
(3) Jiang, M.; Li, M.; Xiang, M.; Zhou, H. *Adv. Polym. Sci.* **1999**, *146*, 121.
(4) Webber, S. E. *J. Phys. Chem. B.* **1998**, *102*, 2618.
(5) (a) Moffitt, M.; Khougaz, K.; Eisenberg, A. *Acc. Chem. Res.* **1996**, *29*, 95. (b) Shen, H. W.; Zhang, L. F.; Eisenberg, A. *J. Am. Chem. Soc.* **1999**, *121*, 2728. (c) Yu, K.; Bartels, C.;

Eisenberg, A. *Macromolecules* **1998**, *31*, 9399. (d) Yu, Y. S.; Zhang, L. F.; Eisenberg, A. *Macromolecules* **1998**, *31*, 1144. (e) Zhang, L. F.; Eisenberg. A. *J. Am. Chem. Soc.* **1996**, *118*, 3168.
(6) (a) Kikuchi, A.; Nose, T. *Macromolecules* **1996**, *29*, 6770. (b) Kikuchi, A.; Nose, T. *Macromolecules* **1997**, *30*, 896.
(7) (a) Liu, F. T.; Liu, G. J. *Macromolecules* **2001**, *34*, 1302. (b) Ding, J. F.; Liu, G. J. *Chem. Mater.* **1998**, *10*, 537.
(8) (a) Jenekhe, S. A.; Chen, X. L. *Science* **1998**, *279*, 1903. (b) Jenekhe, S. A.; Chen, X. L. *Science* **1999**, *283*, 372. (c) Jenekhe, S. A.; Chen, X. L. *J. Phys. Chem. B* **2000**, *104*, 6332. (d) Chen, X.; Jenekhe, S. *Macromolecules* **2000**, *33*, 4610.
(9) (a) Liu, S.; Jiang, M.; Liang, H.; Wu, C. *Polymer* **2000**, *41*, 8697. (b) Liu, S.; Jiang, M. *Chem. J. Chin. Univ.* **2001**, *22*, 1066. (c) Wang, M.; Zhang, G.; Chen, D.; Jiang, M.; Liu, S. *Macromolecules* **2001**, *34*, 7172. (d) Yuan, X.; Jiang, M.; Zhao, H.; Wang, M.; Zhao, Y.; Wu, C. *Langmuir* **2001**, *17*, 6122. (e) Zhao, H.; Liu, S.; Jiang, M.; Yuan, X.; An, Y.; Liu, L. *Polymer* **2000**, *41*, 2705. (f) Zhao, H.; Gong, J.; Jiang, M.; An, Y. *Polymer* **1999**, *40*, 4521. (g) Yuan, X.; Zhao, H.; Jiang, M.; An, Y. *Acta Chim. Sin.* **2000**, *58*, 118. (h) Liu, S.; Jiang, M. *Chem. J. Chin. Univ.* **2001**, *22*, 1066 (i) Zhu H.; Yuan, X.; Zhao, H.; Liu S.; Jiang, M. *Chin. J. Appl. Chem.* **2001**, *18*, 336.
(10) Duan, H.; Chen, D.; Jiang, M.; Gan, W.; Li, S.; Wang, M.; Gong, J. *J. Am. Chem. Soc.* **2001**, *123*, 12097.
(11) Meier, M. *Chem. Soc. Rev.* **2000**, *29*, 295.
(12) (a) Caruso, F.; Caruso, R. A.; Mohwald, H. *Science* **1998**, *282*, 1111. (b) Caruso, F.; Caruso, R. A.; Mohwald, H. *Chem. Mater.* **1999**, *11*, 3309.
(13) Mandal, T. K.; Fleming, M. S.; Walt, D. R. *Chem. Mater.* **2000**, *12*, 3481.
(14) (a) Marinakos, S. M.; Novak, J. P.; Brousseau, L. C., III; Blaine House, A.; Ekedi, E. M.; Feldhaus, J. C.; Feldheim, D. L. *J. Am. Chem. Soc.* **1999**, *121*, 8518. (b) Marinakos, SM.; Anderson, M. F.; Ryan, J. A.; Martin, L. D.; Feldheim, D. L. *J. Phys. Chem. B* **2001**, *105*, 8872.
(15) (a) Ding, J.; Liu, G. *Chem. Mater.* **1998**, *10*, 537. (b) Ding, J.; Liu, G. *J. Phys. Chem. B* **1998**, *102*, 6107. (c) Stewart, S.; Liu, G. *Chem. Mater.* **1999**, *11*, 1048.
(16) (a) Huang, H.; Kowalewski. T.; Remsen, E.; Gertzmann, R.; Wooley, K. L. *J. Am. Chem. Soc.* **1997**, *119*, 11653. (b) Huang, H.; Remsen, E.; Kowalewski. T.; Wooley, K. L. *J. Am. Chem. Soc.* **1999**, *121*, 3805. (c) Zhang, Q.; Remsen, E.; Wooley, K. L. *J. Am. Chem. Soc.* **2000**, *122*, 3642.
(17) Sanji, T.; Nakatsuka, Y.; Ohnishi, S.; Sakurai, H. *Macromolecules* **2001**, *33*, 8524.
(18) Stewart, S.; Liu, G. J. *Angew. Chem., Int. Ed.* **2000**, *39*, 340.
(19) Lee, HK.; Lee, H.; Ko, Y. H.; Chang, Y. J.; Oh, NK.; Zin, WC.; Kim, K. *Angew. Chem., Int. Ed.* **2001**, *40*, 2669.
(20) (a) Qiu, X.; Jiang, M. *Polymer*, **1994**, *35*, 5084. (b) Qiu, X.; Jiang, M. *Polymer*, **1995**, *36*, 3601. (c) Zhou, H.; Xiang, M.; Chen, W.; Jiang, M. *Macromol. Chem. Phys.* **1997**, *198*, 809.
(21) Coleman, M.; Painter, P. *Prog. Polym. Sci.* **1995**, *20*, 1.
(22) (a) Zhu, L.; Jiang, M.; Liu, L.; Zhou, H.; Fan, L.; Zhang, Y. *J. Macromol. Sci., Phys.* **1998**, *B37(6)*, 805. (b) Zhu, L.; Jiang, M.; Liu, L.; Zhou, H.; Fan, L.; Zhang, Y.; Wu, C. *J. Macromol. Sci., Phys.* **1998**, *B37*, 827. (c) Xiang, M.; Jiang, M.; Zhang, Y.; Wu, C.; Feng, L. *Macromolecules* **1997**, *30*, 2313.
(23) Mortensen, K.; Talmon, Y,; Gao, B.; Kops, J. *Macromolecules* **1997**, *30*, 6764.
(24) Zhang, G.; Niu, A.; Peng, S.; Jiang, M.; Tu, Y.; Li. M.; Wu, C. *Acc. Chem. Res.* **2001**, *34*, 249.
(25) Bartels, C. R. EP 0 470 699 A1.
(26) Frechet, J. M. J.; Meftahi, M. V. D. *Br. Polym. J.* **1984**, *16*, 193.
(27) (a) Thurmond, K. B., II; Kowalewski, T.; Wooley, K. L. *J. Am. Chem. Soc.* **1996**, *118*, 7398. (b) Thurmond, K. B., II; Kowalewski, T.; Wooley, K. L. *J. Am. Chem. Soc.* **1997**, *119*, 6656.
(28) Zhang, G.; Liu, L.; Zhao, Y.; Ning, F.; Jiang, M.; Wu, C. *Macromolecules* **2000**, *33*, 6340.
(29) Mössmer, M.; Spatz, J.; Möller, M.; Aberle, T.; Schmidt, J.; Burchard, W. *Macromolecules*, **2000**, *33*, 4791.
(30) Donath, E.; Sukhorukov, G. B.; Caruso, F.; Davis, S. A.; Mohwold, H. *Angew. Chem., Int. Ed. Engl.* **1998**, *37*, 2202.
(31) Jiang, P.; Bertone, J. E.; Colvin, V. L. *Science* **2001**, *291*, 453.
(32) Chu, B. *Laser Light Scattering: Basic Principles and Practice,* 2nd ed.; Academic Press: New York, 1991.
(33) (a) Cao, X.; Jiang, M.; Yu, T. *Makromol. Chem.* **1989**, *190*, 117. (b) Liu, S.; Zhu, H.; Zhao, H.; Jiang, M.; Wu, C. *Langmuir* **2000**, *16*, 3712.

MA0201330